Journal of Neurochemistry, 2007, **101**, 241–249 doi:10.1111/j.1471-4159.2006.04361.x

Mitochondrial dysfunction in Huntington's disease: the bioenergetics of isolated and *in situ* mitochondria from transgenic mice

Jorge M. A. Oliveira,*[,1] Mika B. Jekabsons,*[,2] Sylvia Chen,* Amy Lin,* A. Cristina Rego,† Jorge Gonçalves,‡[,1] Lisa M. Ellerby* and David G. Nicholls*

*Buck Institute for Age Research, Novato, California, USA

†Center for Neuroscience and Cell Biology, University of Coimbra, Coimbra, Portugal

‡Department of Pharmacology, University of Porto, Porto, Portugal

Abstract

Mitochondrial dysfunction is believed to participate in Huntington's disease (HD) pathogenesis. Here we compare the bioenergetic behavior of forebrain mitochondria isolated from different transgenic HD mice (R6/2, YAC128 and *Hdh*150 knock-in) and wild-type littermates with the first determination of *in situ* respiratory parameters in intact HD striatal neurons. We assess the Ca^{2+}-loading capacity of isolated mitochondria by steady Ca^{2+}-infusion. Mitochondria from R6/2 mice (12–13 weeks) and 12 months YAC128, but not homozygous or heterozygous *Hdh*150 knock-in mice (15–17 weeks), exhibit increased Ca^{2+}-loading capacity when compared with respective wild-type littermates. *In situ* mitochondria in intact striatal neurons show high respiratory control. Moreover, moderate expression of full-length mutant huntingtin (in *Hdh*150 knock-in heterozygotes) does not significantly impair mitochondrial respiration in unstimulated neurons. However, when challenged with energy-demanding stimuli (NMDA-receptor activation in pyruvate-based media to accentuate the mitochondria role in Ca^{2+}-handling), *Hdh*150 neurons are more vulnerable to Ca^{2+}-deregulation than neurons from their wild-type littermates. These results stress the importance of assessing HD mitochondrial function in the cellular context.

Keywords: calcium, excitotoxicity, Huntington's disease, *in situ* respiration, mitochondria, striatal neurons.

J. Neurochem. (2007) **101**, 241–249.

Huntington's disease (HD) is a hereditary neurodegenerative disorder caused by a mutation in the gene encoding huntingtin (Htt). Mutant Htt contains an abnormal polyglutamine (polyQ) expansion, responsible for deleterious effects (HDCRG 1993). Despite similar expression levels throughout the brain, mutant Htt selectively targets striatal neurons, with the cerebral cortex being affected later in the disease (Vonsattel and DiFiglia 1998). Mitochondrial dysfunction likely contributes to HD pathogenesis (Beal 2005), and may underlie the selective neuronal degeneration.

Mitochondrial dysfunction in HD was proposed to stem from a direct interaction with mutant Htt (Panov *et al.* 2002), decreasing mitochondrial Ca^{2+}-loading capacity and thus rendering neurons more vulnerable to Ca^{2+}-mediated excitotoxicity. However, studies of mitochondrial Ca^{2+}-loading capacity in HD have provided conflicting results. Decreased Ca^{2+}-loading capacity was observed in mitochondria isolated from immortalized lymphocytes (lymphoblasts) of HD patients, brains of YAC72 HD

Received August 7, 2006; revised manuscript received September 29, 2006; accepted October 2, 2006.

Address correspondence and reprint requests to Prof. David Nicholls or Lisa M. Ellerby, Buck Institute for Age Research, 8001 Redwood Blvd., Novato, California USA. E-mail: dnicholls@buckinstitute.org or lellerby@buckinstitute.org

[1]The present address of Jorge M. A. Oliveira and Jorge Gonçalves is the Department of Pharmacology, Faculty of Pharmacy, University of Porto, 4050-047 Porto, Portugal.

[2]The present address of Mika B. Jekabsons is the Department of Biology, University of Mississippi, 1110 Shoemaker Hall, University, Mississippi 38677, USA.

Abbreviations used: $[Ca^{2+}]_e$, extra-mitochondrial Ca^{2+} concentration; $[Ca^{2+}]_i$, intracellular Ca^{2+} concentration; BSA, bovine serum albumin; CaG5 N, Calcium Green 5 N; DIV, days *in vitro*; FCCP, carbonylcyanide-*p*-(trifluoromethoxyphenyl) hydrazone; HD, Huntington's disease; *Hdh*, mouse HD gene; Htt, huntingtin; NMDAR, NMDA receptor; polyQ, polyglutamine; PT, permeability transition; RCR, respiratory control ratio; $TMRM^+$, tetramethylrhodamine methyl ester; YAC, yeast artificial chromosome.$\Delta\psi_m$, mitochondrial membrane potential.

mice (Panov *et al.* 2002), and livers of knock-in HD mice (Choo *et al.* 2004). In contrast, increased Ca^{2+}-loading capacity was observed in isolated brain mitochondria from R6/2 and knock-in HD mice (Brustovetsky *et al.* 2005). Hence, changes in the Ca^{2+}-loading capacity of HD mitochondria remain controversial and thus require further evaluation. Moreover, as most functional studies have been performed with mitochondria isolated from their cellular context, how HD affects *in situ* mitochondrial function, namely in the vulnerable striatal neurons, remains largely unknown.

Mitochondria can only accumulate Ca^{2+} until the onset of permeability transition (PT). Because experimental conditions strongly influence PT onset (Chalmers and Nicholls 2003) and may account for some of the discrepancies in the literature concerning the Ca^{2+}-loading capacity of HD mitochondria, in the present work, we adopt strategies to study mitochondrial Ca^{2+}-loading capacity independently from other potential bioenergetic differences. Thus, Ca^{2+} was slowly infused (Zoccarato and Nicholls 1982) into a dilute mitochondrial suspension supplemented with adenine nucleotides. A previous study with rat brain mitochondria (Chalmers and Nicholls 2003) showed that this provided a highly reproducible measure of Ca^{2+}-loading capacity by minimizing bioenergetic demands on the mitochondria that result in depolarization or NAD(P)H oxidation.

In the present study, we assess the Ca^{2+}-loading capacities of forebrain mitochondria isolated from three different transgenic HD mouse models. We find an increased Ca^{2+}-loading capacity in mitochondria from R6/2 and YAC128 mice, but not in those from homozygous or heterozygous *Hdh*150 knock-in mice. Having failed to detect Ca^{2+}-handling abnormalities with isolated mitochondria from knock-in mice, we tested for selective mitochondrial dysfunction in intact striatal neurons that might have been concealed in the mixture of neuronal and glial mitochondria isolated from the forebrain.

In this study, we present the first determination of *in situ* mitochondria respiratory function in intact HD striatal neurons, using a previously described technique (Jekabsons and Nicholls 2004) that avoids many of the artifacts inherent to isolated mitochondrial preparations. We find that *in situ* mitochondria show surprisingly high respiratory control, and that moderate expression of mutant Htt (in *Hdh*150 knock-in heterozygous) does not significantly impair mitochondrial respiration, at least in resting young neurons. However, when we challenge *in situ* mitochondria with high Ca^{2+}, by transiently activating NMDA receptors, we find that *Hdh*150 striatal neurons fail to reestablish Ca^{2+} homeostasis in higher proportion, when compared with neurons from wild-type littermates. These results stress the importance of assessing HD mitochondria function *in situ*, i.e., in the appropriate cellular context.

Materials and methods

Materials

Calcium Green 5 N (CaG5 N), tetramethylrhodamine methyl ester ($TMRM^+$) and Fluo-5F AM were from Molecular Probes (Eugene, OR, USA). Culture media and supplements were purchased from Invitrogen (Carlsbad, CA, USA). NMDA, (5R,10S)-(+)-5-methyl-10,11-dihydro [a,d] cyclohepten -5,10-imine hydrogen maleate, myxothiazol, oligomycin, rotenone, carbonylcyanide-*p*-(trifluoromethoxyphenyl) hydrazone (FCCP) and other reagents were from Sigma (St. Louis, MO, USA).

Mouse forebrain mitochondria

Transgenic mice

All procedures involving animals were performed in accordance with the Institutional Animal Care and Use Committee guidelines. Twelve-to-thirteen-week-old R6/2 (Mangiarini *et al.* 1996), 52–55 week-old YAC128 (Slow *et al.* 2003) and 15–17 week-old *Hdh*150 knock-in HD transgenic mice (Lin *et al.* 2001) and respective wild-type littermates (backgrounds: B5CBAF1/J, FVB/N and C57BL/6 J, respectively) were used in this study. R6/2 mice express a short N-terminal fragment of human Htt with ~150 polyQ, in addition to wild-type mouse Htt (Mangiarini *et al.* 1996), presenting rapid disease onset and early death when compared with HD mice expressing full-length Htt (Hickey and Chesselet 2003). YAC128 mice (line 53) express full-length human Htt with 128 polyQ by means of a yeast artificial chromosome (YAC), in addition to wild-type mouse Htt (Slow *et al.* 2003). Knock-in mice are a faithful reproduction of the HD genotype as the elongated polyQ tracts are encoded within the correct context of the mouse *Hdh* gene (Hickey and Chesselet 2003), homologous to the human HD gene. *Hdh*150 knock-in mice (CHL2 line) encode full-length Htt with 150 polyQ either in a single allele (heterozygous, $Hdh^{150/+}$) or in both alleles (homozygous, $Hdh^{150/150}$) (Lin *et al.* 2001). The wild-type littermates of these knock-in mice are hereafter designated by $Hdh^{+/+}$.

Isolation

Mitochondria were isolated from mouse forebrain (brain minus cerebellum). The cerebellum was excluded as it is usually not involved in HD pathology (Vonsattel and DiFiglia 1998). Similar to previous studies about mitochondrial Ca^{2+}-loading capacity in HD transgenic mice (Panov *et al.* 2002; Brustovetsky *et al.* 2005), percoll gradient centrifugation (Sims 1990) was used to prepare non-synaptosomal mitochondria (see Appendix S1 for details).

Mitochondrial Ca^{2+} accumulation and membrane potential

Mitochondria (0.2 mg of protein) were suspended in 2 mL of incubation buffer (10 mmol/L NaCl, 90 mmol/L KCl, 20 mmol/L HEPES pH 7.2, 0.1% fatty acid free bovine serum albumin (BSA), 5 mmol/L succinate, 2 mmol/L Na_2HPO_4, 0.2 mmol/L ADP and 5 μg/mL oligomycin) containing $TMRM^+$ at 1 μmol/L (quench mode, Chalmers and Nicholls 2003) and 0.2 μmol/L CaG5 N for simultaneous monitoring of respective changes in mitochondrial membrane potential ($\Delta\psi_m$) and extra-mitochondrial Ca^{2+} concentration ($[Ca^{2+}]_e$). Paired experiments were performed at 37°C using two alternating stirred cuvettes in the automated four-position turret of a Perkin-Elmer LS-50B fluorimeter (Wellesley, MA, USA).

$CaCl_2$ infusions were performed at a steady rate of 21 nmol/mg/min with a Braun Perfusor (FT Scientific Instruments, Glos., Tewksbury, UK) modified to take a pair of 100 μL Hamilton microsyringes (Zoccarato and Nicholls 1982). CaG5 N was excited at 506 nm and emission collected at 532 nm. Changes in $\Delta\psi_m$ were followed qualitatively by the fluorescence quenching of $TMRM^+$ (549 nm excitation, 575 nm emission).

Cultured striatal neurons

Cell culture

Primary striatal cultures were generated from the offspring of crosses between two heterozygous *Hdh*150 mice or between a heterozygous male and a wild-type female from the same genetic background (C57BL/6 J). Brains from E16-17 embryos were rapidly removed into ice-cold Hank's balanced salt solution, while tails and livers were collected for PCR genotyping (Fig. S1a). The genotyping procedure, requiring DNA purification, was not sufficiently fast to allow for brain pooling. Therefore, the entire culture procedure was performed in parallel for individual brains, resulting in 'single-embryo striatal cultures' plated blindly to genotype. Briefly, striata were dissected, minced with a scalpel and dissociated with 0.25% trypsin-EDTA. After enzyme inhibition with 10% heat-inactivated fetal bovine serum in Neurobasal medium, cells were plated onto 8-well chambered coverglasses (LabTek, Naperville, IL, USA) at a density of 2.5×10^5 cells per well, or onto 22 × 40-mm glass coverslips at a density of 1×10^6 cells per coverslip. The glass was previously coated with 33 μg/mL polyethyleneimine. Cultures were maintained in Neurobasal medium supplemented with 1% glutamax, 2% B27, 1% fetal bovine serum, 100 U/mL penicillin and 0.1 μg/mL streptomycin. Two days after plating, 10 μmol/L cytosine arabinoside was added to inhibit growth of glial cells. After 4 days *in vitro* (DIV), cells were fed by replacing half the culture media. At 9 DIV glucose was added to a final concentration of 15 mmol/L using a 1.6 mol/L stock solution. Cultures were maintained at 37°C in a 95/5% air/CO_2 incubator and used for experiments at 10–13 DIV. Normal and mutant Htt expression in neuronal cultures was confirmed by western blotting (Fig. S1b).

Cell respirometer

Measurements of oxygen uptake by intact coverslip-attached neurons using a 'cell respirometer' were previously described in detail (Jekabsons and Nicholls 2004). Briefly, 22 × 40-mm coverslips with attached neurons were mounted in a perfusion chamber (RC-30; Warner Instruments, Hamden, CT, USA) coupled to two miniature polarographic Clark-type oxygen electrodes (Microelectrodes Inc., Bedford, NH, USA) monitoring the oxygen tension of the solution entering and exiting the chamber. Perfusion media was composed by (in mmol/L): 120 NaCl, 3.5 KCl, 0.4 KH_2PO_4, 1.3 $CaCl_2$, 5 $NaHCO_3$, 1.2 Na_2SO_4, 20 TES, 15 glucose, 10 pyruvate, 0.4% fatty acid free BSA, pH 7.4 at 37°C.

Functional confocal microscopy

Single-cell imaging of neurons, plated in 8-well Lab-Tek chambers, was performed in a Zeiss Pascal confocal Axiovert 100 M inverted microscope (Thornwood, NY, USA) using a 20 × air objective (at 0.7 zoom) and argon (488 nm) and helium-neon (543 nm) lasers. For the simultaneous monitoring of changes in intracellular Ca^{2+} concentration ($[Ca^{2+}]_i$) and $\Delta\psi_m$, cells were loaded with 0.5 μmol/L Fluo-5F AM, $K_d(Ca^{2+})$ = 2.3 μmol/L, and 50 nmol/L $TMRM^+$ (quench mode, Nicholls and Ward 2000) for 30 min at 37°C in incubation buffer containing (in mmol/L): 120 NaCl, 3.5 KCl, 0.4 KH_2PO_4, 1.3 $CaCl_2$, 20 TES, 5 $NaHCO_3$, 1.2 Na_2SO_4, 15 glucose (pH 7.4). At the end of the incubation, cells were washed thrice with fresh incubation buffer containing 50 nmol/L $TMRM^+$ with glucose replaced by 10 mmol/L pyruvate in order to accentuate the mitochondrial role in the maintenance of Ca^{2+} homeostasis. Experiments were performed in this buffer at 37°C. Cells were excited at 488 nm for Fluo-5F (emission 505–530) and at 543 nm for $TMRM^+$ (emission > 560 nm). Individual cell somata were identified as regions of interest for the determination of fluorescence time-courses. NMDA receptor activation was achieved with 100 μmol/L NMDA/10 μmol/L glycine in the absence of Mg^{2+}. After 10 min, MK801 (5 μmol/L) was added to block receptor activation and allow for neuronal recovery.

Results

Mitochondrial Ca^{2+}-loading capacity from different Huntington's disease mouse models during steady Ca^{2+}-infusion

In this study, we compare the Ca^{2+}-loading capacity of forebrain mitochondria isolated from different transgenic HD mice (R6/2, YAC128 and *Hdh*150 knock-in) and respective wild-type littermates. Mitochondrial Ca^{2+}-loading capacity was estimated by a continuous Ca^{2+}-infusion procedure (Zoccarato and Nicholls 1982), avoiding the bioenergetic demands that result from Ca^{2+}-bolus addition. Also, a diluted mitochondrial suspension was used (0.1 mg/mL) to avoid premature propagation of the permeability transition (premature PT) by a sub-population of susceptible mitochondria releasing sufficient Ca^{2+} to trigger a 'chain-reaction' overload and PT in adjacent mitochondria, which may cause to underestimate the Ca^{2+}-loading capacity of the overall population (Chalmers and Nicholls 2003). Real-time changes in extramitochondrial Ca^{2+} concentration, $[Ca^{2+}]_e$, and $\Delta\psi_m$ were simultaneously monitored throughout the experiments.

Addition of mitochondria to the incubation medium reduces $[Ca^{2+}]_e$, as the residual cation in the media is taken up by the organelle, and decreases $TMRM^+$ fluorescence because of probe uptake and quenching in the matrix (Fig. 1a). The onset of Ca^{2+}-infusion (at 21 nmol/mg/min) increases $[Ca^{2+}]_e$ into a plateau, as the Ca^{2+} accumulating activity of the mitochondrial uniporter gets in balance with both the infusion rate and the mitochondrial Ca^{2+}-efflux pathway (Zoccarato and Nicholls 1982; Chalmers and Nicholls 2003). Mitochondria continuously accumulate Ca^{2+}, buffering $[Ca^{2+}]_e$, until a steep rise occurs (Fig. 1a). This steep $[Ca^{2+}]_e$ rise reflects the occurrence of PT in the mitochondrial population and is delayed approximately twofold if 1 μmol/L cyclosporin A is present (not shown). When compared to the $[Ca^{2+}]_e$ rise, the increase in $TMRM^+$ fluorescence is earlier and less steep. This is because in the

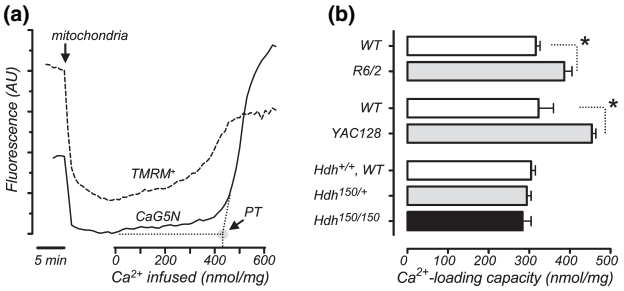

Fig. 1 Ca^{2+}-loading capacity of forebrain mitochondria isolated from Huntington's disease mice. Simultaneous monitoring of mitochondrial Ca^{2+}accumulation with Calcium Green 5 N (CaG5 N) and mitochondrial membrane potential with tetramethylrhodamine methyl ester ($TMRM^+$) was performed as described under Materials and methods. (a) Representative tracings are from an experiment with YAC128 mitochondria. Tracings obtained with mitochondria from other experimental groups were qualitatively similar. Addition of mitochondria (arrow) leads to the uptake of residual Ca^{2+} and $TMRM^+$ quenching in the matrix. After signal stabilization, $CaCl_2$ was continuously infused at a steady rate of 21 nmol/mg/min. Mitochondria accumulate Ca^{2+} until the onset of permeability transition (PT, estimated by the interception of the dotted lines), evidenced by a steep $[Ca^{2+}]_e$ rise. AU, arbitrary units. (b) Mean ± SEM of mitochondrial Ca^{2+}-loading capacity, $n = 4$ for all experimental groups, except $n = 2$ for $Hdh^{+/+}$ and $Hdh^{150/150}$ mice. Mitochondria from wild-type (WT) mice of the three different background strains present similar Ca^{2+}-loading capacities (white bars). Mitochondria from either R6/2 or YAC128 mice (but not from $Hdh^{150/+}$ or $Hdh^{150/150}$ mice) accumulate more Ca^{2+} compared with the respective WT littermates (*$p < 0.05$, paired *t*-test).

course of Ca^{2+} infusion a fraction of the mitochondria undergoes early PT, collapsing $\Delta\psi_m$, decreasing the aggregate matrix volume and causing Ca^{2+} and $TMRM^+$ release (and thus $TMRM^+$ dequenching, which increases its fluorescence). While Ca^{2+} release is buffered to a specific set-point by uniporter reuptake into the polarized mitochondria, the reuptake of $TMRM^+$ is governed by Nernst equilibrium and hence does not match what is released by the fraction of the mitochondria undergoing early PT because of the decrease in aggregate matrix volume (Chalmers and Nicholls 2003). Thus, the assessment of mitochondrial Ca^{2+}-loading capacity by monitoring the rise in $[Ca^{2+}]_e$ (Fig. 1a) is a better estimate of the overall mitochondrial population, than the monitoring of the distribution of $\Delta\psi_m$ sensitive probes such as $TMRM^+$.

A comparison of mitochondrial Ca^{2+}-loading capacity for different HD mouse models is shown in Fig. 1b. Irrespective of the genetic background, mitochondria from wild-type mice exhibit a similar Ca^{2+}-loading capacity (316 ± 15, 323 ± 37 and 305 ± 11 nmol/mg for the wild-type littermates of R6/2, YAC128 and *Hdh*150 knock-in mice, respectively (Fig. 1b – white bars). Interestingly, mitochondria from both R6/2 and YAC128 mice present an increased Ca^{2+}-loading capacity (386 ± 27 and 454 ± 10 nmol/mg for R6/2 and YAC128, respectively; *$p < 0.05$ vs. wild-type littermates). This effect is not apparent in *Hdh*150 knock-in animals where Ca^{2+}-loading capacities were similar to wild-type littermates (294 ± 11 and 284 ± 21 nmol/mg, for heterozygous and homozygous animals, respectively). It should be noted that R6/2 mice at ~12 weeks, as used in the present study, are resistant to quinolinic acid injection in the striatum (Hansson *et al.* 2001), and both cortical and striatal mitochondria have increased glutathione levels (Choo *et al.* 2005), compatible with the observed increase in mitochondrial Ca^{2+}-loading capacity, in agreement with previous findings (Brustovetsky *et al.* 2005). Also, YAC128 mice at the age used in the present study (~12 months) present cortical and striatal atrophy associated with striatal neuronal loss (Slow *et al.* 2003), and cognitive dysfunction (Van Raamsdonk *et al.* 2005), supportive of ongoing HD neuropathology and hence compatible with our observation of abnormal mitochondrial Ca^{2+}-handling.

In contrast, knock-in HD mice usually have less widespread pathology than other genetic HD models (Hickey and Chesselet 2003). $Hdh^{150/150}$ and less frequently $Hdh^{150/+}$ mice have behavioral and gait abnormalities starting at 15 weeks of age (Lin *et al.* 2001), suggesting ongoing HD neuropathology at the age used in the present study (15–17 weeks). To the best of our knowledge, there are no previous studies with brain mitochondria from *Hdh*150 knock-in mice. However, abnormalities in striatal but not cortical mitochondria Ca^{2+}-handling have been reported at ~12 weeks for other knock-in mice with shorter Htt polyQ tracts (Brustovetsky *et al.* 2005). Hence, it is possible that the mixed neuronal glial population of the forebrain might have concealed a dysfunction selective for striatal neurons in *Hdh*150 knock-in mice. Therefore, and having in mind the faithful reproduction of the HD genotype in knock-in mice (Hickey and Chesselet 2003), we studied *in situ* mitochondrial function in cultured striatal neurons from these mice.

In situ mitochondrial respiration in striatal neurons from $Hdh^{150/+}$ knock-in mice and wild-type littermates

Using a cell respirometer (Jekabsons and Nicholls 2004), we monitored *in situ* mitochondrial respiration of intact coverslip-attached striatal neurons from heterozygous *Hdh*150 knock-in mice ($Hdh^{150/+}$) and wild-type ($Hdh^{+/+}$) littermates (Fig. 2). In each experiment, we compared an $Hdh^{+/+}$ with an $Hdh^{150/+}$ from the same litter. We tested three pairs of littermates ($n = 3$ experiments), each pair deriving from a different litter. Four respiratory rates were measured: basal (V_{basal}), maximal uncontrolled respiration in the presence of 9 μmol/L FCCP (V_{FCCP}), oligomycin (0.2 μg/mL)-insensitive (V_{oligo}), and residual non-mitochondrial respiration ($V_{rot/myx}$) in the presence of 1 μmol/L rotenone plus 2 μmol/L mixothiazol (oligomycin maintained after V_{oligo} assessment).

The *in situ* mitochondrial respiration accounts for ~91% of basal respiration [$(V_{basal} - V_{rot/myx})/V_{basal} = 90.7 \pm 0.4\%$

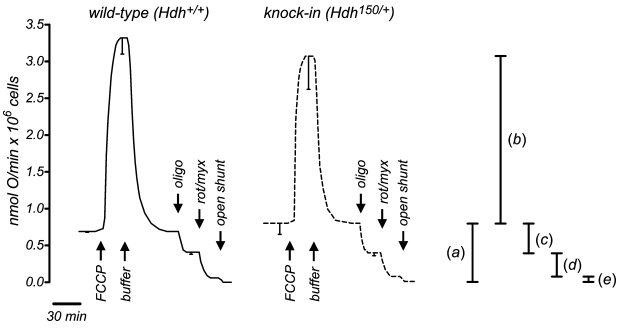

Fig. 2 *In situ* respiration of mitochondria in striatal neuronal cultures from Huntington's disease mice. Monitoring of oxygen uptake by intact coverslip-attached cells was performed as described under Materials and methods to determine: (a) basal respiration, (b) reserve ATP-generating capacity, (c) respiration supporting ATP turnover, (d) respiration driving mitochondrial H^+ leak, and (e) non-mitochondrial respiration. Basal respiration was determined prior to perfusion with 9 μmol/L carbonylcyanide-*p*-(trifluoromethoxyphenyl) hydrazone (FCCP) to assess maximal respiration. After 1 h of recovery in standard buffer, cells were sequentially perfused with 0.2 μg/mL oligomicyn (oligo) and with 1 μmol/L rotenone plus 2 μmol/L myxothiazol (rot/myx). At the end of the experiment, the downstream oxygen electrode received buffer bypassing the chamber (open shunt) to correct for electrode drift and assess nonmitochondrial respiration. Results are mean ± SEM of three independent experiments.

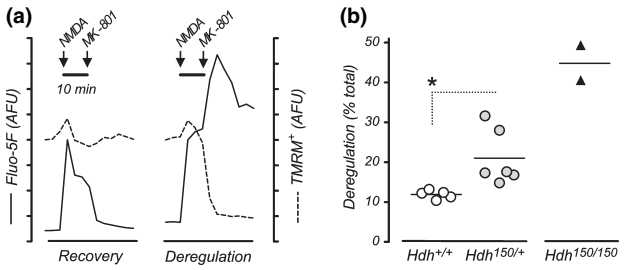

Fig. 3 Susceptibility to NMDA receptor (NMDAR) activation in pyruvate media of striatal neurons from *Hdh*150 knock-in mice. Simultaneous monitoring of changes in neuronal $[Ca^{2+}]_i$ with Fluo-5F and mitochondrial membrane potential with tetramethylrhodamine methyl ester ($TMRM^+$) was performed as described under Materials and methods. (a) Representative tracings of single neurons exhibiting 'recovery' (left) or 'deregulation' (right), following NMDAR activation (see Results for a detailed description). AFU, arbitrary fluorescence units. (b) Each circle represents the percentage of neurons that exhibited 'deregulation' in cultures from different embryos (white circles, $Hdh^{+/+}$, $n = 5$; gray circles, $Hdh^{150/+}$, $n = 6$) deriving from three different litters. $Hdh^{150/+}$ neurons were more prone to undergo 'deregulation' than $Hdh^{+/+}$ neurons (*$p < 0.05$, unpaired *t*-test). Black triangles are two separate determinations using two sister cultures from the same homozygous ($Hdh^{150/150}$) embryo.

for $Hdh^{+/+}$ and 90.5 ± 2.2% for $Hdh^{150/+}$]. In the basal state, mitochondria are respiring only at about 1/5 of maximal capacity $[(V_{basal} - V_{rot/myx})/(V_{FCCP} - V_{rot/myx}) = 19.3 \pm 1.1\%$ for $Hdh^{+/+}$ and 23.5 ± 1.6% for $Hdh^{150/+}$]. Also, only a minor percentage of the total ATP generating capacity is used in the basal state $[(V_{basal} - V_{oligo})/(V_{FCCP} - V_{oligo}) = 9.8 \pm 1.3\%$ for $Hdh^{+/+}$ and 14.4 ± 1.8% for $Hdh^{150/+}$], with approximately half of the basal mitochondrial respiration driving H^+ leaks across the mitochondrial inner membrane $[(V_{oligo} - V_{rot/myx})/(V_{basal} - V_{rot/myx}) = 55.0 \pm 3.7\%$ for $Hdh^{+/+}$ and 45.8 ± 3.2% for $Hdh^{150/+}$].

In situ mitochondria from both genotypes show high pseudo-respiratory control ratios [(state 3 FCCP/state 4) $= (V_{FCCP} - V_{rot/myx})/(V_{oligo} - V_{rot/myx}) = 9.50 \pm 0.22$ for $Hdh^{+/+}$ and 9.38 ± 0.03 for $Hdh^{150/+}$]. Thus, at this young age, the presence of a single mutant allele encoding Htt in the $Hdh^{150/+}$ mice does not significantly impair mitochondrial respiration, at least in resting striatal neurons. Still, it cannot be excluded that the trend for a higher basal respiration and ATP turnover, as well as for a smaller maximal respiratory capacity in $Hdh^{150/+}$ neurons may represent early signs of dysfunction.

Susceptibility to NMDA-receptor activation of striatal neurons from *Hdh*150 knock-in mice

Having observed no major effect of mutant Htt expression on mitochondrial respiration of resting $Hdh^{150/+}$ striatal neurons, we asked whether challenging of *in situ* mitochondria with energy-demanding stimuli, such as high $[Ca^{2+}]_i$, might reveal differences unapparent under resting conditions. To address this question, we assessed the ability of striatal neurons to re-establish neuronal homeostasis following transient NMDA-receptor (NMDAR) activation (Fig. 3). NMDAR activation leads to massive Ca^{2+}-entry, threatening neuronal survival. Mitochondria play an important role in the maintenance of neuronal homeostasis, both by taking up Ca^{2+} and synthesizing ATP required for energy-dependent homeostatic mechanisms. To accentuate this mitochondrial role, we performed experiments in media with pyruvate (10 mmol/L) instead of glucose. Under these conditions, neurons depend on ATP derived solely from oxidative phosphorylation, thus accentuating the bioenergetic consequences of mitochondrial dysfunction. Indeed, if mitochondrial Ca^{2+}-uptake and ATP synthesis are prevented (treatment with 1 μmol/L rotenone plus 2 μg/mL oligomycin), striatal neurons fail to recover from NMDAR activation (not shown).

Changes in neuronal homeostasis were estimated by the dynamic monitoring of changes in $[Ca^{2+}]_i$ and $\Delta\psi_m$ by fluorescence microscopy with Fluo-5F and $TMRM^+$. A 10 min challenge with 100 μmol/L NMDA / 10 μmol/L glycine, followed by receptor blockade with 5 μmol/L (5R,10S)-(+)-5-methyl-10,11-dihydro [A,D] cyclohepten -5,10-imine hydrogen maleate, permitted the distinction between striatal neurons able to re-establish cellular homeostasis ('recovery') and those that underwent intracellular Ca^{2+} deregulation associated with $\Delta\psi_m$ collapse ('deregulation'), a condition that is well correlated with necrotic cell

death (Nicholls and Budd 2000; Fig. 3a). For each experiment, we analyzed the responses from 250 individual neurons and calculated the percentage unable to recover from NMDAR activation, i.e., exhibiting 'deregulation' (Fig. 3b).

Expression of mutant huntingtin increases the proportion of striatal neurons unable to recover from NMDAR activation. 11.9 ± 0.5% of wild-type ($Hdh^{+/+}$, 1250 neurons analyzed) versus 21.0 ± 2.8% of heterozygous *Hdh*150 knock-in striatal neurons ($Hdh^{150/+}$, 1500 neurons analyzed) exhibit 'deregulation' following NMDAR activation (five vs. six embryos from three different litters; $*p < 0.05$ unpaired *t*-test with Welch's correction for unequal variances; Fig. 3b).

Obtaining homozygous *Hdh*150 embryos ($Hdh^{150/150}$) with wild-type littermates was a difficult task as it required the mating of two heterozygous animals and the killing of pregnant transgenic females. In addition, not all heterozygous × heterozygous crosses yielded homozygous progeny. We managed to collect functional data from two separately assayed sister cultures from the same $Hdh^{150/150}$ embryo and observed a percentage of 44.8 ± 4.4% of striatal neurons (500 neurons analyzed) exhibiting 'deregulation' following NMDAR activation. It is noteworthy that this percentage is higher than in any of the individual experiments performed with neurons from $Hdh^{+/+}$ and $Hdh^{150/+}$ embryos, and that the entire neuronal culture procedure and plating was blinded to genotype.

Discussion

Here, we have assessed the Ca^{2+}-loading capacity of isolated forebrain mitochondria from three different transgenic HD mice. Using experimental conditions that prevent premature PT propagation by mitochondrial sub-populations, i.e., the use of low mitochondrial concentrations and the inclusion of adenine nucleotides in the incubation, we find that wild-type mitochondria from three different genetic backgrounds present similar Ca^{2+}-loading capacities. In contrast, Ca^{2+}-loading capacity is increased in forebrain mitochondria isolated from R6/2 and YAC128 HD mice, but not in those from *Hdh*150 knock-in mice with less severe pathology. When focusing on neurons selectively targeted by HD, we find that moderate mutant Htt expression, in $Hdh^{150/+}$ striatal neurons, does not significantly impair *in situ* mitochondrial respiration. However, when *in situ* mitochondria are challenged with high Ca^{2+} by transient NMDAR activation, mutant Htt expression is associated with a higher proportion of striatal neurons failing to re-establish Ca^{2+} homeostasis. We conclude that in order to understand more deeply how mitochondrial function is affected in HD, studies need to be conducted not only with isolated mitochondria but also with *in situ* mitochondria.

Functional assays with HD mitochondria have mostly been performed with the isolated organelle (Panov *et al.* 2002; Choo *et al.* 2004; Brustovetsky *et al.* 2005). As isolation removes mitochondria from the cytoplasm, extrapolations to *in vivo* HD are limited. Moreover, as non-synaptosomal brain preparations (Panov *et al.* 2002; Brustovetsky *et al.* 2005) are inevitably contaminated with glial mitochondria and are depleted in synaptic mitochondria, both neuronal-selective and synaptic dysfunction will be obscured. Hence, despite considerable progress, several fundamental questions raised by isolated mitochondria studies remain unsettled or yet to be addressed by studying *in situ* HD mitochondria.

Considering the conflicting results previously obtained with isolated HD mitochondria (Panov *et al.* 2002; Choo *et al.* 2004; Brustovetsky *et al.* 2005), the effects of mutant Htt on mitochondrial Ca^{2+}-handling are still debatable. Brustovetsky *et al.* (2005) reported an age-dependent increase in the Ca^{2+}-loading capacity of striatal but not of cortical mitochondria isolated from HD mice. In no instance did Brustovetsky *et al.* (2005) observe a decreased Ca^{2+}-loading capacity for HD mitochondria, in contrast to earlier reports for HD brain mitochondria and for liver and lymphoblast HD mitochondria (Panov *et al.* 2002; Choo *et al.* 2004). The approximately 3–6-fold variation in mitochondrial concentration between these studies is noteworthy [0.16 mg/mL (Brustovetsky *et al.* 2005) vs. 0.5 mg/mL (Panov *et al.* 2002) and 1 mg/mL (Choo *et al.* 2004)], because high concentrations increase the possibility that a minor subset of susceptible mitochondria might trigger early PT in the overall population, underestimating the Ca^{2+}-loading capacity of the major population. Our present data, using a slow Ca^{2+}-infusion into a diluted (0.1 mg/mL) mitochondrial suspension to minimize this premature PT propagation, are consistent with an increased Ca^{2+}-loading capacity in the overall HD mitochondria population. Hence, at least for HD brain mitochondria, the opposing results could be reconciled assuming that the majority of the population does acquire enhanced resistance to Ca^{2+} loads (Brustovetsky *et al.* 2005), but that they include a small yet vulnerable fraction that can trigger premature PT in the population if high mitochondrial concentrations are used (Panov *et al.* 2002). While a deleterious interaction with mutant Htt may explain why some HD mitochondria are more vulnerable to Ca^{2+} (Panov *et al.* 2002, 2003), possible reasons behind the 'population resistance' are less straightforward. Increased mitochondrial resistance may result from adaptive responses to a stressful environment, as previously proposed (Brustovetsky *et al.* 2005).

An apparent increase in brain mitochondria resistance to Ca^{2+} over-load could derive from the fact that isolated brain mitochondria are an inevitable mixture of neuronal and glial mitochondria and that these mitochondria differ (Bambrick *et al.* 2004; Kristian *et al.* 2005). As neuronal loss in HD is accompanied by glial proliferation (Myers *et al.* 1991), a decreased neuron/glia ratio could account for increased

resistance of the mitochondrial population without adaptive changes in individual mitochondria. Indeed, neuronal loss and/or gliosis have been described for several HD mouse models (Reddy *et al.* 1998; Lin *et al.* 2001; Slow *et al.* 2003; Yu *et al.* 2003), but even non-lethal neuronal atrophy by itself could decrease the neuron/glia mitochondria ratio if the number of mitochondria per neuron decreases. Development of assays that allow a reliable and independent analysis of neuronal and glial mitochondria Ca^{2+}-handling is essential to resolve this issue. So far, the only method that allows the isolation of pure neuronal versus glial mitochondria is to use primary cultures (Kristian *et al.* 2005).

The present study is, to the best of our knowledge, the first to assess *in situ* HD mitochondrial respiratory function in intact (non-permeabilized) coverslip-attached neurons from transgenic mice. A recent study (Milakovic and Johnson 2005) monitored mitochondrial respiration in immortalized striatal progenitor cells obtained from wild-type mice (ST*Hdh*$^{+/+}$ cells, expressing wild-type Htt), and from homozygous knock-in HD mice (ST*Hdh*$^{111/111}$ cells, expressing mutant Htt with 111 polyQ) (Trettel *et al.* 2000). The immortalized cells were permeabilized with digitonin, an approach that allows the access of non-cell permeant reagents to the mitochondria inside the cells, permitting a comprehensive analysis of mitochondrial respiration but unavoidably leading to dialysis of soluble cytosolic components, and thus being bioenergetically equivalent to an isolated mitochondrial preparation.

Milakovic and Johnson (2005) reported that mitochondrial respiration and ATP production were significantly impaired in ST*Hdh*$^{111/111}$ cells when compared with ST*Hdh*$^{+/+}$ cells, however, neither significant differences were found in the activity of the mitochondrial respiratory complexes, nor in the total ATP cellular levels. The authors suggest that in intact cells, under resting conditions, mitochondria are likely not to function at maximal capacity and that only under conditions of neuronal stress would the mitochondrial impairment contribute to HD pathogenesis. Here we demonstrate that in intact striatal neurons, under resting conditions, mitochondria are indeed working at submaximal capacity. Furthermore, we show that under neuronal stress (NMDAR activation), when ATP is deriving solely from the mitochondria (pyruvate media), expression of full-length mutant Htt is associated with an increased vulnerability to Ca^{2+}-deregulation. Our single-cell measurements suggest that this vulnerability is only restricted to a subset rather than to a uniform impairment of the neuronal population. This is consistent with the large *in situ* mitochondrial spare respiratory capacity of the neuronal population expressing mutant Htt. While no significant change in spare respiratory capacity argues against respiratory chain impairment, defects in ATP synthesis and/or export in HD neurons cannot be excluded.

Our *in situ* respiration data contrast with that of Milakovic and Johnson (2005), first by the absence of significant differences in mitochondrial respiration, and second by much higher respiratory control ratios (RCR) in the present study. The fact that ST*Hdh*$^{111/111}$ cells express two copies of mutant Htt versus only one in *Hdh*$^{150/+}$ striatal neurons is a likely explanation for the first difference. Indeed, despite HD patients with two mutant alleles being very rare, evidence supports that homozygosity is associated with a more severe clinical course (Squitieri *et al.* 2003), also, mouse studies show a clear gene dosage effect (Hickey and Chesselet 2003). As both mutant and wild-type Htt associate with the mitochondria (Choo *et al.* 2004), depletion of wild-type Htt because of homozygosity of the mutation may also play an important role (Cattaneo *et al.* 2001; Zhang *et al.* 2003). Concerning differences in RCR values, which were ≤ 4 for the ST*Hdh* cell lines (both for state3/state4 or state3/uncoupled ratios, irrespective of the substrates) (Milakovic and Johnson 2005) and approximately 9–10 for striatal neurons in the present study, they may result both from differences in methodology and in the mitochondrial origin.

We could not find any published RCR data for brain mitochondria of HD mice. However, they are expected to be low based on available data from wild-type mouse brain isolated mitochondria [RCR = 1.6–2.0 (Lobao-Soares *et al.* 2005); 2.82 ± 0.13 (Xu *et al.* 2001); > 2 were used in experiments (Levy *et al.* 2003); and an exception of 7.5 ± 0.4 (Chavez *et al.* 1995)]. Interestingly, a comparative study with rat mitochondria isolated from different tissues (Rossignol *et al.* 2000) reported the lowest RCR for the brain (2.6 ± 1.4), when compared with muscle, heart, liver and kidney. Significantly, mitochondria isolated from cultured rat neurons with a recently improved methodology presented RCRs of approximately 9–10 (Kristian *et al.* 2005). Moreover, our observation of mitochondria respiring at only $\sim$1/5 of maximal capacity in the basal state, is consistent with $\sim$500% spare respiratory capacity for *in situ* mitochondria in synaptosomes (Nicholls and Budd 2000). Thus, it is likely that *in situ* neuronal mitochondria present more robust respiratory properties than commonly isolated brain mitochondria.

In summary, the present study shows an overall increase in the Ca^{2+}-loading capacity of forebrain mitochondria from R6/2 and YAC128 HD mice. Because of limitations in the use of isolated non-synaptosomal preparations, it is presently unclear whether this represents a true mitochondrial resistance or changes in the neuronal/glial mitochondria ratio. Failure to observe such resistance in *Hdh*150 knock-in mice may be related to the slower progression of the disease in these mice and/or the concealment of a striatal selective effect in the forebrain mitochondria population. Studies of mitochondrial respiration in intact heterozygous *Hdh*150 striatal neurons reveal no significant defects in spare respiratory capacity, basal ATP synthesis, or uncoupling and do not support a uniform major bioenergetic defect in

these neurons. Still, when the bioenergetic demand is strong, such as during NMDAR activation, a select population of HD striatal neurons may be unable to meet the increased ATP demand, perhaps because of defects in ATP synthesis/export. Additional studies, addressing *in situ* mitochondrial function in HD neurons and glial cells will be of importance to understand HD pathogenesis.

Acknowledgements

This work was supported by NIH grant NS40251A (LME), NINDS grant RO1 NS04 1908 (DGN), the HighQ Foundation (ACR, LME and JMAO) and the Calouste Gulbenkian Foundation (JMAO). We thank Dr Michael Hayden for the YAC128 mice and Dr Detloff for the HD150 knockin mice.

Supplementary material

The following supplementary material is available for this article:

Appendix S1. Further details regarding mitochondrial isolation and western analysis.

Fig. S1 Genotyping of *Hdh*150 knock-in mice and huntingtin expression in cultured striatal neurons.

This material is available as part of the online article from http://www.blackwell-synergy.com

References

Bambrick L., Kristian T. and Fiskum G. (2004) Astrocyte mitochondrial mechanisms of ischemic brain injury and neuroprotection. *Neurochem. Res.* **29**, 601–608.

Beal M. F. (2005) Mitochondria take center stage in aging and neurodegeneration. *Ann. Neurol.* **58**, 495–505.

Brustovetsky N., LaFrance R., Purl K. J., Brustovetsky T., Keene C. D., Low W. C. and Dubinsky J. M. (2005) Age-dependent changes in the calcium sensitivity of striatal mitochondria in mouse models of Huntington's Disease. *J. Neurochem.* **93**, 1361–1370.

Cattaneo E., Rigamonti D., Goffredo D., Zuccato C., Squitieri F. and Sipione S. (2001) Loss of normal huntingtin function: new developments in Huntington's disease research. *Trends Neurosci.* **24**, 182–188.

Chalmers S. and Nicholls D. G. (2003) The relationship between free and total calcium concentrations in the matrix of liver and brain mitochondria. *J. Biol. Chem.* **279**, 19 062–19 070.

Chavez J. C., Pichiule P., Boero J. and Arregui A. (1995) Reduced mitochondrial respiration in mouse cerebral cortex during chronic hypoxia. *Neurosci. Lett.* **193**, 169–172.

Choo Y. S., Johnson G. V., MacDonald M., Detloff P. J. and Lesort M. (2004) Mutant huntingtin directly increases susceptibility of mitochondria to the calcium-induced permeability transition and cytochrome c release. *Hum. Mol. Genet.* **13**, 1407–1420.

Choo Y. S., Mao Z., Johnson G. V. and Lesort M. (2005) Increased glutathione levels in cortical and striatal mitochondria of the R6/2 Huntington's disease mouse model. *Neurosci. Lett.* **386**, 63–68.

Hansson O., Guatteo E., Mercuri N. B., Bernardi G., Li X. J., Castilho R. F. and Brundin P. (2001) Resistance to NMDA toxicity correlates with appearance of nuclear inclusions, behavioural deficits and changes in calcium homeostasis in mice transgenic for exon 1 of the huntington gene. *Eur. J. Neurosci.* **14**, 1492–1504.

HDCRG (1993) A novel gene containing a trinucleotide repeat that is expanded and unstable on Huntington's disease chromosomes. The Huntington's Disease Collaborative Research Group. *Cell* **72**, 971–983.

Hickey M. A. and Chesselet M. F. (2003) The use of transgenic and knock-in mice to study Huntington's disease. *Cytogenet. Genome Res.* **100**, 276–286.

Jekabsons M. B. and Nicholls D. G. (2004) *In situ* respiration and bioenergetic status of mitochondria in primary cerebellar granule neuronal cultures exposed continuously to glutamate. *J. Biol. Chem.* **279**, 32 989–33 000.

Kristian T., Hopkins I. B., McKenna M. C. and Fiskum G. (2005) Isolation of mitochondria with high respiratory control from primary cultures of neurons and astrocytes using nitrogen cavitation. *J. Neurosci. Methods* **152**, 136–143.

Levy M., Faas G. C., Saggau P., Craigen W. J. and Sweatt J. D. (2003) Mitochondrial regulation of synaptic plasticity in the hippocampus. *J. Biol. Chem.* **278**, 17 727–17 734.

Lin C. H., Tallaksen-Greene S., Chien W. M., Cearley J. A., Jackson W. S., Crouse A. B., Ren S., Li X. J., Albin R. L. and Detloff P. J. (2001) Neurological abnormalities in a knock-in mouse model of Huntington's disease. *Hum. Mol. Genet.* **10**, 137–144.

Lobao-Soares B., Bianchin M. M., Linhares M. N. *et al.* (2005) Normal brain mitochondrial respiration in adult mice lacking cellular prion protein. *Neurosci. Lett.* **375**, 203–206.

Mangiarini L., Sathasivam K., Seller M. *et al.* (1996) Exon 1 of the HD gene with an expanded CAG repeat is sufficient to cause a progressive neurological phenotype in transgenic mice. *Cell* **87**, 493–506.

Milakovic T. and Johnson G. V. (2005) Mitochondrial respiration and ATP production are significantly impaired in striatal cells expressing mutant huntingtin. *J. Biol. Chem.* **280**, 30 773–30 782.

Myers R. H., Vonsattel J. P., Paskevich P. A., Kiely D. K., Stevens T. J., Cupples L. A., Richardson E. P. Jr and Bird E. D. (1991) Decreased neuronal and increased oligodendroglial densities in Huntington's disease caudate nucleus. *J. Neuropathol. Exp. Neurol.* **50**, 729–742.

Nicholls D. G. and Budd S. L. (2000) Mitochondria and neuronal survival. *Physiol. Rev.* **80**, 315–360.

Nicholls D. G. and Ward M. W. (2000) Mitochondrial membrane potential and cell death: mortality and millivolts. *Trends Neurosci.* **23**, 166–174.

Panov A. V., Gutekunst C. A., Leavitt B. R., Hayden M. R., Burke J. R., Strittmatter W. J. and Greenamyre J. T. (2002) Early mitochondrial calcium defects in Huntington's disease are a direct effect of polyglutamines. *Nat. Neurosci.* **5**, 731–736.

Panov A. V., Burke J. R., Strittmatter W. J. and Greenamyre J. T. (2003) *In vitro* effects of polyglutamine tracts on Ca^{2+}-dependent depolarization of rat and human mitochondria: relevance to Huntington's disease. *Arch. Biochem. Biophys.* **410**, 1–6.

Reddy P. H., Williams M., Charles V., Garrett L., Pike-Buchanan L., Whetsell W. O. Jr, Miller G. and Tagle D. A. (1998) Behavioural abnormalities and selective neuronal loss in HD transgenic mice expressing mutated full-length HD cDNA. *Nat. Genet.* **20**, 198–202.

Rossignol R., Letellier T., Malgat M., Rocher C. and Mazat J. P. (2000) Tissue variation in the control of oxidative phosphorylation: implication for mitochondrial diseases. *Biochem. J.* **347**, 45–53.

Sims N. R. (1990) Rapid isolation of metabolically active mitochondria from rat brain and subregions using Percoll density gradient centrifugation. *J. Neurochem.* **55**, 698–707.

Slow E. J., van Raamsdonk J., Rogers D. *et al.* (2003) Selective striatal neuronal loss in a YAC128 mouse model of Huntington disease. *Hum. Mol. Genet.* **12**, 1555–1567.

Squitieri F., Gellera C., Cannella M. *et al.* (2003) Homozygosity for CAG mutation in Huntington disease is associated with a more severe clinical course. *Brain* **126**, 946–955.

Trettel F., Rigamonti D., Hilditch-Maguire P., Wheeler V. C., Sharp A. H., Persichetti F., Cattaneo E. and Macdonald M. E. (2000) Dominant phenotypes produced by the HD mutation in STHdh(Q111) striatal cells. *Hum. Mol. Genet.* **9**, 2799–2809.

Van Raamsdonk J. M., Pearson J., Slow E. J., Hossain S. M., Leavitt B. R. and Hayden M. R. (2005) Cognitive dysfunction precedes neuropathology and motor abnormalities in the YAC128 mouse model of Huntington's disease. *J. Neurosci.* **25**, 4169–4180.

Vonsattel J. P. and DiFiglia M. (1998) Huntington disease. *J. Neuropathol. Exp. Neurol.* **57**, 369–384.

Xu G. P., Dave K. R., Moraes C. T., Busto R., Sick T. J., Bradley W. G. and Pérez-Pinzón M. A. (2001) Dysfunctional mitochondrial respiration in the wobbler mouse brain. *Neurosci. Lett.* **300**, 141–144.

Yu Z. X., Li S. H., Evans J., Pillarisetti A., Li H. and Li X. J. (2003) Mutant huntingtin causes context-dependent neurodegeneration in mice with Huntington's disease. *J. Neurosci.* **23**, 2193–2202.

Zhang Y., Li M., Drozda M. *et al.* (2003) Depletion of wild-type huntingtin in mouse models of neurologic diseases. *J. Neurochem.* **87**, 101–106.

Zoccarato F. and Nicholls D. G. (1982) The role of phosphate in the regulation of the Ca efflux pathway of liver mitochondria. *Eur. J. Biochem.* **127**, 333–338.

